

Extrasolar Binary Planets I: Formation by tidal capture during planet-planet scattering

H. Ochiai¹, M. Nagasawa², and S. Ida³

1) *Earth and Planetary Sciences, Tokyo Institute of Technology, 2-12-1 Ookayama, Meguro-ku, Tokyo 152-8551, Japan*

2) *Interactive Research Center of Science, Tokyo Institute of Technology, 2-12-1, Ookayama, Meguro-ku, Tokyo 152-8551, Japan*

3) *Earth-Life Science Institute, Tokyo Institute of Technology, 2-12-1 Ookayama, Meguro-ku, Tokyo 152-8550, Japan*

nagasawa.m.ad@m.titech.ac.jp

ABSTRACT

We have investigated i) the formation of gravitationally bounded pairs of gas-giant planets (which we call "binary planets") from capturing each other through planet-planet *dynamical* tide during their close encounters and ii) the following long-term orbital evolution due to planet-planet and planet-star *quasi-static* tides. For the initial evolution in phase i), we carried out N-body simulations of the systems consisting of three jupiter-mass planets taking into account the dynamical tide. The formation rate of the binary planets is as much as 10 % of the systems that undergo orbital crossing and this fraction is almost independent of the initial stellarcentric semi-major axes of the planets, while ejection and merging rates sensitively depend on the semi-major axes. As a result of circularization by the planet-planet dynamical tide, typical binary separations are a few times the sum of the physical radii of the planets. After the orbital circularization, the evolution of the binary system is governed by long-term quasi-static tide. We analytically calculated the quasi-static tidal evolution in later phase ii). The binary planets first enter the spin-orbit synchronous state by the planet-planet tide. The planet-star tide removes angular momentum of the binary motion, eventually resulting in a collision between the planets. However, we found that the binary planets survive the tidal decay for main-sequence life time of solar-type stars (~ 10 Gyrs), if the binary planets are beyond ~ 0.3 AU from the central stars. These results suggest that the binary planets can be detected by transit observations at $\gtrsim 0.3$ AU.

Subject headings: planets and satellites: formation — dynamical evolution and stability — detection

1. INTRODUCTION

About a half of the discovered extrasolar gas-giant planets have eccentric orbits with eccentricity $e \gtrsim 0.2$. Planet-planet scattering is one of the relevant mechanisms to excite their eccentricities after the formation of the gas giants. Early studies on this subject (e.g., Rasio & Ford 1996; Weidenschilling & Marzari 1996) assumed two gas giants with initially close enough orbital separations for them to start orbital crossing quickly. However, it may not be easy to realize such or-

bitally unstable orbital configurations as a result of their formation processes. On the other hand, systems of three gas giants with modest orbital separations start orbital crossing as a result of long-term secular perturbations well after the formation of the systems, such systems have been regarded as more plausible initial conditions and they have been intensively studied by later papers (e.g., Lin & Ida 1997; Marzari & Weidenschilling 2002; Chatterjee et al. 2008; Jurić & Tremaine 2008). During the orbital crossing, the planets repeatedly undergo close encounters and their ec-

centricities are highly pumped up. Typical fates of the three planet systems are ejections of a planet, planet-planet collisions, and planet-star collisions. Through these events, usually the remaining two planets acquire widely separated eccentric orbits and further orbital crossing does not occur.

In the simulations that include planet-star tidal interactions, the gravitational scatterings can lead to formation of hot jupiters. If the eccentricity of a planet is excited up to ~ 1 , the pericenter becomes very close to the host star. Then, the tidal dissipation of the planet induced by the star (dynamical tide) damps its semi-major axis and eccentricity and the planet becomes a hot jupiter (Rasio & Ford 1996). Nagasawa et al. (2008) and Beaugé & Nesvorný (2012) investigated the orbital evolution of the three gas-giant planets systems that initially have circular orbits beyond the snow line, by N-body simulations including the planet-star tidal interaction. Although most of the hot jupiters fall inside of the stellar Roche radius due to subsequent tidal decay during timescales of the order of 1 Gyr (Beaugé & Nesvorný 2012), the previous papers found that hot jupiters are formed in as much as 10-30% of the systems that undergo orbital crossing.

The tidal dissipation also occurs between closely encountering two planets. So, there is another possibility of the fate of planet-planet scattering, that is, formation of binary planets. This possibility has not been studied in the planet-planet scattering scenarios. Podsiadlowski et al. (2010) studied the formation of binary planets in extrasolar planetary systems for the first time and demonstrated that binary planets can be actually formed from two gas giant planets in 1–20% of the runs at 0.2–5AU, by orbital calculations including planet-planet tidal interactions.

However, Podsiadlowski et al. (2010) started calculations from two gas giant planets in almost circular orbits with the orbital separation between the two planets of $\sim 2.4r_{\text{Hill}}$, where r_{Hill} is the Hill radius. As mentioned in the above, these unstable orbital configurations would not be established in real systems, and this initial condition may make trapping of binary planets easier. With this conditions, the planets immediately undergo close encounters before their eccentricities are pumped up. As a result, the close encounters have relatively low relative velocity in this case, and the trapping

probability is higher for lower relative velocity.

Dynamical behaviors in two planet systems are qualitatively different from that with three planets or more. While close encounters cannot occur in the two planet systems unless their orbital separation is smaller than $2\sqrt{3}r_{\text{Hill}}$ (Gladman 1993), the three planet systems do not have such a solid stability boundary. With modest initial orbital separations, the three planet systems can start orbital crossing after their eccentricities are built up on relatively long timescales (e.g., Chambers et al. 1996). Note that such dynamical behavior is similar even if the number of planets is increased from three. Although it is not clear how much fraction of planetary systems actually become unstable after the gas disk dispersal (e.g., Lega et al. 2013), calculations starting from three planets in modestly separated orbits would be much more appropriate than that from two planets in packed circular orbits, in order to evaluate the formation rate of binary gas giant planets in extrasolar planetary systems. In a separate paper (Ochiai et al. 2014, which we refer to Paper II), we will discuss the detectability of binary planets by transit observations. For such discussions, statistical results based on simulations of planet-planet scattering of three planets are more helpful than those with two planets.

In this paper, we carry out N-body simulations of systems of three giant planets, taking account of planet-planet interactions by dynamical tide as well as planet-star ones to simulate tidal capture of the planets with each other and circularization of the captured orbits. In §2, we describe basic equations of the N-body simulation and the model for the dynamical tide that is incorporated in the N-body simulation. In §3, we present the numerical results. We show that the formation rate of the binary planets is as high as $\sim 10\%$ almost independent of stellarcentric semimajor axis in the three planet system. After orbital circularization due to dynamical tide, the evolution of the binary system is governed by long-term quasi-static tide. We analytically calculate the long-term tidal orbital evolution of the formed binary planets during main-sequence phase lifetimes of central stars. Section 4 is the conclusions.

2. METHODS

2.1. Basic equations of N-body simulation

We consider the planetary systems, which are composed of a central star and three gas giant planets. We take the origin of the coordinate at the central star with mass M_* . The equation of motion of planet i is

$$\frac{d^2 \mathbf{r}_i}{dt^2} = -G \frac{M_* + M_i}{r_i^3} \mathbf{r}_i - GM_j \left(\frac{\mathbf{r}_j}{r_j^3} + \frac{\mathbf{r}_{ij}}{r_{ij}^3} \right) - GM_k \left(\frac{\mathbf{r}_k}{r_k^3} + \frac{\mathbf{r}_{ik}}{r_{ik}^3} \right), \quad (1)$$

where M_i and \mathbf{r}_i are masses and position vectors of planet i ($= 1, 2, \text{ and } 3$), respectively, and $\mathbf{r}_{ij} \equiv \mathbf{r}_i - \mathbf{r}_j$.

When a planet passes the pericenter to the star or another planet, we impulsively dissipate the orbital energy of the passing bodies according to tidal interactions, following Nagasawa & Ida (2011). We impose the tidal interactions with the host star only for encounters with the stellarcentric pericenter distance $q < 0.04$ AU to save computational time.

When a planet repeatedly undergoes close encounters with the central star and suffers the tidal dissipation, its semimajor axis and orbital eccentricity shrink keeping q almost constant (e.g., Nagasawa et al. 2008; Nagasawa & Ida 2011). As a result, the planet becomes a hot jupiter.

If a planet encounters another planet closely enough, the planets can be trapped through planet-planet tidal dissipation to form a gravitationally bound pair. At the initial phase after the trapping, eccentricity of the binary orbit is generally close to unity. Through repeated encounters, the binary orbit is circularized in a similar way to the formation of hot jupiters. Since the relative motion is described by hyperbolic orbits at the trapping, and by highly eccentric orbits in most of time during the circularization, the tidal interaction is dominated by dynamical tide, which is described in the following.

2.2. Tidal dissipation between planets

For tidal trapping and circularization of binary orbits, we use the formula for energy loss

due to dissipation due to dynamical tide between two objects derived by Portegies Zwart & Meinen (1993), following Podsiadlowski et al. (2010). When planet i and j undergo tidal interactions, the tidal energy loss caused by a single close encounter between the planets is

$$E_{\text{tide}} = \frac{GM_j^2}{R_i} \left[\left(\frac{R_i}{q_{ij}} \right)^6 T_2(\eta_i) + \left(\frac{R_i}{q_{ij}} \right)^8 T_3(\eta_i) \right] + \frac{GM_i^2}{R_j} \left[\left(\frac{R_j}{q_{ij}} \right)^6 T_2(\eta_j) + \left(\frac{R_j}{q_{ij}} \right)^8 T_3(\eta_j) \right], \quad (2)$$

where q_{ij} is the pericenter distance between planet i and j , R_i is planetary physical radius, $\eta_i \equiv \{M_i/(M_i + M_j)\}^{1/2} (q_{i,j}/R_i)^{3/2}$, and $T_{2,3}(\eta_i)$ are given by Portegies Zwart & Meinen (1993) as a fifth-degree polynomial function.

For encounters between the planets with the pericenter distance less than $10(R_i + R_j)$, we subtract tidal dissipation energy from their orbital energy at the pericenter passage using impulse approximation. Because tidal interactions rapidly weaken as the distance between the bodies increases, even if we switch on the tidal interaction at larger distance, the results hardly change (see §3.2).

Strictly speaking, it may not be correct to use the impulse approximation and equation (2) after the eccentricity of the binary orbit is significantly damped, because the oscillation of the planetary bodies raised by the tides is not dissipated before the next encounter. In such situations, how the semi-major axis and eccentricity of the binary orbit are changed by dynamical tides depends on the phase of oscillation, and a and e change chaotically (e.g., Press & Teukolsky 1977; Mardling 1995). However, we are most concerned with early phase of the tidal trapping to evaluate the formation probability of binary planets. So, we neglect the chaotic evolution due to incomplete oscillation damping.

Note that the formulas for dynamical tide could include large uncertainty, because the effect of dynamical tide depends on what wave modes are excited and how they dissipate. However, the tidal dissipation energy is inversely proportional to several powers of mutual distance between the planets. In the case of equation (2), $E_{\text{tide}} \propto q_{ij}^{-6}$. Even if E_{tide} changes by a factor 10, the capture separation changes only by 50%.

case	a_1 (AU)	R_i (R_J)	binary planets	collision	HJs	ejection	3 remain
set 1	1	2	8	68	8	16	0
set 3	3	2	10	30	17	41	2
set 5	5	2	9	32	20	38	1
set 10	10	2	13	15	16	54	2
set 0.5a	0.5	1	9	64	12	15	0
set 3a	3	2,1,1	17	23	23	37	0
set 3b	3	2	6	41	15	33	0
set 5a	5	2	8	34	16	42	0

Table 1: The parameters and results of 8 sets of N-body simulations of three gas giant planets. Each set includes 100 runs with different initial orbital phases. The parameter a_1 is the initial stellarcentric semimajor axis of the innermost planet and R_i is the physical radius of the planets in unit of Jovian radius R_J . The rows "binary planets", "collision", "HJs", and "ejection" refer to the number of runs that end up with formation binary planets, planet-planet and planet-star collisions, formation of hot jupiters through tidal circularization, and ejection from the systems, respectively. The last row represents the number of runs in which orbital interaction of three planets continues until the end of calculations (10 Myrs).

After the circularization, quasi-static tides become predominant instead of dynamical tides. Although quasi-static tides are weaker by orders of magnitude than dynamical tides for high orbital eccentricity, quasi-static tides work also for circular binary orbits and last until spin-orbit synchronous state is established. Thus the cumulative effect in orbital evolution due to quasi-static tide is important when we consider observational detectability of binary planets. In §3.4, we calculate such longer-term tidal evolution due to quasi-static tides between planets, taking into account planetary spins and also tides between the planets and the host star. The formulation is based on tidal dissipation functions Q , instead of eq. (2), as explained in Appendix A. We discuss orbital stability against tidal evolution due to quasi-static tides during main sequence lifetime of solar-type host stars (~ 10 Gyrs). We will show that a binary system is stable if stellarcentric distance is $\gtrsim 0.3$ - 0.4 AU. Also note that as long as the tidal capture occurs beyond ~ 0.3 AU from the central star, envelope removal due to the tidal dissipation do not take place (see §3.2).

2.3. Initial conditions

To evaluate the formation rate of the binary planets, we set three giant planets. In early studies, planet-planet scattering simulations started from two planet systems, but recent simulations are all done using three planets or more (e.g.,

Beaugé & Nesvorný 2012).

However, since the pioneering work, Podsiadlowski et al. (2010), carried out two planet simulations as one set of runs, we also performed the same two planet simulations to confirm that our simulation code reproduces the Podsiadlowski et al. (2010)'s results. For each semimajor axis, we carried out 20-30 runs. We found that in the *two planet* cases, the formation rate of binary planets are 1 out of 20 at 0.2 AU, 5 out of 20 at 1.0 AU, and 11 out of 30 at 5.0 AU, respectively. The results are consistent with Podsiadlowski et al. (2010)'s, although the numbers of our runs are smaller than theirs.

Our main results in this paper are obtained by *three planet* simulations. We use initial conditions as follows: the semi-major axes of three planets are $1.0a_1$, $1.45a_1$, and $1.9a_1$ and we test four different initial semi-major axis of the innermost planet, $a_1 = 1, 3, 5$, and 10 AU. Initial orbital eccentricities are zero for all the planets, but we set small orbital inclinations as $I_1 = 0.5^\circ$, $I_2 = 1.0^\circ$, and $I_3 = 1.5^\circ$ to ensure three-dimensional motions, following Marzari & Weidenschiling (2002). We set the other angle variables (the longitudes of ascending node, those of pericenter, and the mean longitude) randomly. For different runs with the same a_1 and planetary radii (R_j), we use different seeds for the random number generation. The mass and radius of the central star are $1M_\odot$ and $1R_\odot$, and that of three planets are $1M_J$ and $2R_J$, respectively. Since the orbital crossing and formation of

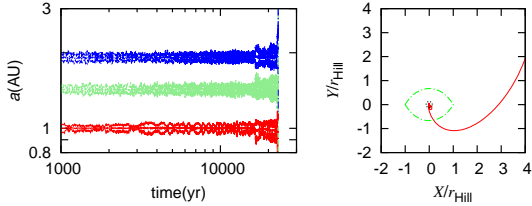


Fig. 1.— An example of orbital evolution to form binary planets. We set $a_1 = 1$ AU. The left panel represents the time evolutions of the semi-major axes. The solid red line, dashed light green line, and dash-dotted blue line are planet 1, 2, and 3, respectively. Two thin lines mean the pericenter distance $a_i(1 - e_i)$ and apocenter distance $a_i(1 + e_i)$. The right panel represents the relative orbit in the Hill coordinate (the solid red line) between planet 2 and 3. The dash-dotted green line and dotted black line indicate the Hill sphere and the region inside which tidal interactions are taken into account, respectively. X and Y are radial and tangential coordinates normalized by the Hill radius.

binary planets may occur at the timings before the envelope of gas giants fully contract, we use relatively large R_i . We also performed additional set of calculations with $a_1 = 0.5$ AU and $R_j = 1R_J$. Unless we particularly note that $R_j = 1R_J$, we use $R_j = 2R_J$ as a nominal parameter (also see Table 1).

For each a_1 , we carried out 100 runs to follow the orbital evolution over 10 Myrs with 4-th order Hermite scheme. We stopped calculations when a pair of planets collide ($r_{ij} \leq R_i + R_j$) or when they form a binary system and the binary eccentricity $e_{\text{bi}} < 0.01$). We regard that a planet is ejected from the system when the instantaneous distance of the planet from the star becomes more than 10000 AU and planet’s eccentricity exceeds unity. We also check the collision between the central star and a planet, but when a planet approaches the central star, it tends to become a hot jupiter due to the tidal interaction with the central star rather than a collision. We neglect spins of the planets and the central star in the N-body simulations for the simplicity (The spin evolution is calculated in the long-term evolution due to quasi-static tide shown in section 3.4).

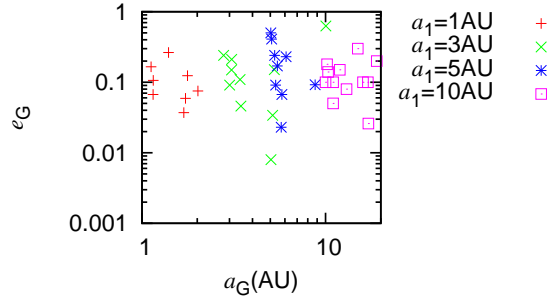


Fig. 2.— The stellarcentric semi-major axes and eccentricities of binary’s centers of mass of four initial $a_1 = 1$ AU (red plus), 3 AU (green cross), 5 AU (blue asterisk), and 10 AU (magenta square).

3. RESULTS

3.1. Distributions of orbital parameters of formed binaries

Figure 1 shows an example of orbital evolution to form a binary of planets. The left panel shows the time evolution of the semi-major axes of the three planets. Two thin lines mean the pericenter distance $a_i(1 - e_i)$ and apocenter distance $a_i(1 + e_i)$. Orbital crossing begins at $t \sim 23000$ yr. Immediately after that, planet 2 (dashed light green line) and 3 (dash-dotted blue line) form a binary.

The right panel represents the path of approaching planets in the local Hill coordinate. The inner planet (planet 2) is set at the origin. In this panel, X axis lies along the line from the central star to the inner planet and Y axis is perpendicular to X . The axes are normalized by Hill radius defined by

$$r_{\text{Hill}} = \left(\frac{M_i + M_j}{3M_*} \right)^{1/3} \frac{M_i a_i + M_j a_j}{M_i + M_j}. \quad (3)$$

The outer planet (denoted by the solid red line) enters the Hill sphere (denoted by the dash-dotted green line) at $t \sim 23000$ yrs. After that two planets undergo repeated close encounters to suffer tidal interactions (dotted black line indicates the region within which tidal interaction is taken into account) for ~ 300 yrs, they form a gravitationally bound pair (binary). We found that when the planet enters the Hill sphere from upper-left

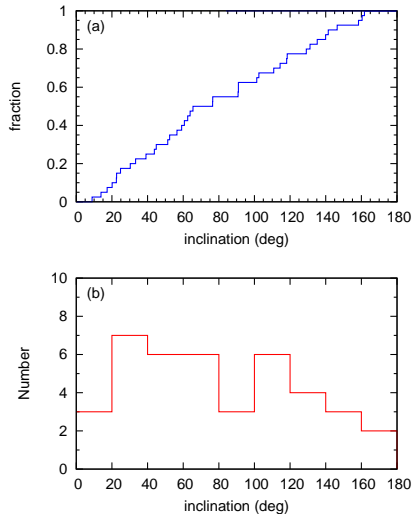


Fig. 3.— The stellarcentric orbital inclinations of binary planets I_{bi} obtained in 400 calculations. This is sum of four initial a_1 in $2R_J$ cases. (a) Cumulative inclination distribution. (b) Histogram of inclination with stride of 20 degrees.

(lower-left) direction in this plot, the planets tend to form a prograde (retrograde) binary.

We present the distribution of the stellarcentric semi-major axes and the eccentricities of binary’s barycenters (a_G and e_G) in Fig. 2. Four different symbols represent the different initial semi-major axes $a_1 = 1$ AU (plus), 3 AU (cross), 5 AU (asterisk), and 10 AU (square). This figure shows that the binary planets are formed near their initial orbits. This is because the binary planets are formed in the early stage of orbital instability before they are significantly diffused by many scatterings. The (stellarcentric) eccentricities of the barycenters of the binary pairs are distributed in the range of 0.01–0.6 with the mean value ~ 0.15 . The mean value corresponds to the eccentricity required for close encounters from initial orbital separation of planets $\sim 4r_{\text{Hill}}$. Since the resultant eccentricities e_G depend on the phase angle of the encounters, they are distributed in a broad range.

Figure 3 shows the stellarcentric orbital inclination of formed binary planets, $I_{\text{bi}} = \arccos(h_{ij,Z}/h_{ij})$, where $h_{ij,Z}$ is the component of $\mathbf{h}_{ij} = \mathbf{r}_{ij} \times \mathbf{v}_{ij}$ that is perpendicular to the orbital plane, and \mathbf{v}_{ij} is the relative velocity between planet i and j . Because we do not see any significant semi-

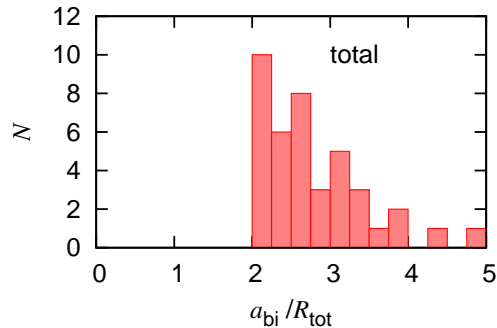


Fig. 4.— The semi-major axis of binary orbits a_{bi} (distance between binaries) obtained in 400 calculations. This is sum of four initial a_1 in $2R_J$ cases.

major axis dependence of I_{bi} , we superpose the results from different initial a_1 . If tidal trapping occurs isotropically, I_{bi} becomes a sine distribution. KS test suggests that this distribution is not the isotropic distribution. The distribution is slightly skewed to small I_{bi} , which might reflect the fact that the trapping occurs in early phase before significant orbital excitations. But, retrograde binary planets are formed in non-negligible fraction of runs (18/40). Note that since we do not take into account the spins of the planets, the retrograde orbits do not necessarily mean the tidally unstable configuration.

Figure 4 shows the final semi-major axis of the binary orbits, a_{bi} . Because we plot the values after the binary eccentricities have been significantly damped ($e_{\text{bi}} < 0.01$), a_{bi} is equivalent to the binary separation. Here we also superpose the results from different initial stellarcentric a_1 . The distribution of a_{bi} is peaked at $2R_{\text{tot}} - 4R_{\text{tot}}$ where $R_{\text{tot}} = R_i + R_j$. This is about twice as large as the pericenter distances just after binary capture (see §3.2). The factor of 2 is attributed to angular momentum conservation during the tidal circularization as below.

Because tidal force is a strong function of a separation distance between two planets, the two planets just after the trapping usually have a highly eccentric binary orbit with $q_{\text{bi},0} \sim R_{\text{tot}} - 2R_{\text{tot}}$. The initial angular momentum of the binary orbit is $h_{\text{bi},0} \simeq [a_{\text{bi},0}(1 - e_{\text{bi},0}^2)]^{1/2} \simeq (2q_{\text{bi},0})^{1/2}$, while the final angular momentum is

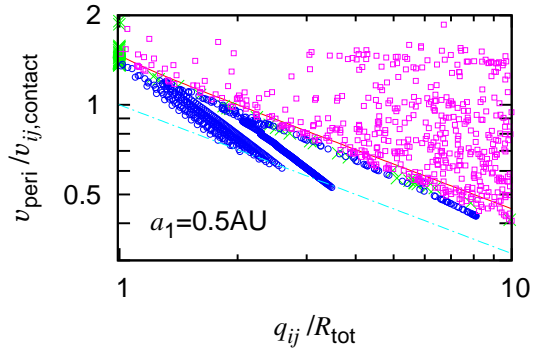


Fig. 5.— The relative distances and velocities at the pericenters of two encountering planets of four initial semi-major axes. The velocities are normalized by the relative velocity of the contact binary. The solid red lines and the dash-dotted light blue lines represent the escape velocity and the Keplerian velocity of the binary planet, respectively. The blue open circles represent pericenter passages of planets that become binaries in the end. Open magenta squares and green crosses show pericenter passages of escaping pairs and colliding pairs, respectively.

$h_{\text{bi}} \simeq a_{\text{bi}}^{1/2}$. The angular momentum conservation indicates that $a_{\text{bi}} \sim 2q_{\text{bi},0}$. This explains the peak at $2 \lesssim a_{\text{bi}}/R_{\text{tot}} \lesssim 4$ and deficit of binary planets at $1 \lesssim a_{\text{bi}}/R_{\text{tot}} \lesssim 2$ in Fig. 4. We found that the peaked value of a_{bi} is much smaller than the Hill radius $\sim 40R_{\text{tot}}$ at 1AU, and the distribution of a_{bi} does not depend on a_1 . This indicates that the binary is hardly affected by interactions with the star or a third planet outside Hill sphere, unless a_G is very small.

3.2. Tidal capture and orbital circularization due to dynamical tide

In this subsection, we show the process of tidal trapping in more details. We assumed that the relative velocity of the planets is impulsively decreased at their closest approach. We expect that the binary planets are formed when the relative velocity (v_{ij}) of two planets immediately after the impulsive tidal dissipation is smaller than their escape velocity,

$$v_{ij} < v_{\text{esc}} = \sqrt{\frac{2G(M_i + M_j)}{r_{ij}}}. \quad (4)$$

In Fig. 5, we present the relative distances (q_{ij}) and the relative velocities (v_{peri}) after the tidal dissipation of two planets at each pericenter passage, in the case of $a_1 = 0.5$ AU with $R_{i,j} = 1R_J$. The velocities are normalized by the relative velocity of the contact binary, $v_{ij,\text{contact}} = [G(M_i + M_j)/R_{\text{tot}}]^{1/2}$, and the pericenter distances are normalized by R_{tot} . When q_{ij}/R_{tot} becomes less than unity, two planets collide. The solid red line represents $v_{\text{peri}} = v_{\text{esc}}$. The passages below this line correspond to those of bound orbits. The dash-dotted (light blue) lines represent the binary’s circular orbital velocity $v_{\text{K,bi}} = [G(M_i + M_j)/r_{ij}]^{1/2}$. When v_{peri} reaches this line, their tidal circularization have been completed. Open blue circles, magenta squares and green crosses represent a series of the pericenter passages of binary, escaping, and colliding pairs, respectively. At points along the line of $v_{\text{peri}} = v_{\text{esc}}$, a binary (a gravitationally bound pair) is first formed. As the binary bodies repeat close approaches, v_{peri} is decreased by tidal dissipation and q_{ij} is increased by the angular momentum conservation, which are represented by a chain of blue open circles from upper-left to lower-right direction in the figure. We found that the first tidal captures of binary planets occur when $q_{ij} \sim R_{\text{tot}} - 2R_{\text{tot}}$, that is, q_{ij} is small enough for the tidal force to be strong enough but larger than R_{tot} to avoid a collision. In all of our simulations, no tidal capture was found from non-bound orbits with $q_{ij} > 3R_{\text{tot}}$ (The blue open circles outside of $4R_{\text{tot}}$ in the figure are wondering passages during the circularization that start from $q_{ij} \sim R_{\text{tot}} - 2R_{\text{tot}}$).

As already mentioned, we included the tidal dissipation when the closest approach occurs within $10R_{\text{tot}}$. As a stellarcentric distance of binary planets increases, the Hill radius becomes larger, but we did not change the threshold distance of $10R_{\text{tot}}$. We carried out extra calculations at $a_1 = 5$ AU with the threshold distance of $50R_{\text{tot}}$, to check its effect (set 5a in Table 1). The formation rate of binary planets is 8 % in this calculations, and binary formation occurred at $q_{ij} > 10R_{\text{tot}}$ in only 1 of 100 runs. So, the results hardly change even if the tidal force is incorporated from more distant encounters than $q_{ij} = 10R_{\text{tot}}$.

Note that tidal destruction of planets hardly occurs in this capture process. The relative velocity at grazing approach ($q_{ij} \sim R_{\text{tot}} - 2R_{\text{tot}}$) that

causes tidal capture, is $v \simeq [v_{\text{gr}}^2 + (ev_{\text{Kep}})^2]^{1/2}$, where ev_{Kep} is relative velocity when the planets are sufficiently separated and v_{gr} is a contribution by the gravitational acceleration between interacting planets, which is given by $\sim (0.5 - 1)v_{\text{esc}}$ for $q_{ij} \sim 2R_{\text{tot}} - 1R_{\text{tot}}$. For nominal parameters, $1M_{\text{J}}$ and $2R_{\text{J}}$, the surface escape velocity is $v_{\text{esc}} \simeq 44\text{km/s}$. The Keplerian velocity is $v_{\text{Kep}} \simeq 30(a/1\text{AU})^{-1/2}\text{km/s}$. Since typical stellarcentric eccentricity is $e \lesssim 0.3$ at the capture (Fig. 4), v_{gr} is dominated and $v \sim (0.5 - 1)v_{\text{esc}}$ for $a \gtrsim 0.3\text{AU}$, where the orbits of binary planets are stable on timescales of ~ 10 Gyrs (see section 3.4). For collision cases, SPH simulation (e.g., Ikoma et al. 2006) showed that significant envelope loss occurs only for $v \gtrsim 2v_{\text{esc}}$. Therefore, the tidal destruction is unlikely.

The tidal dissipation could inflate the planetary envelope, which accelerates tidal circularization. However, while this may change total circularization timescale, it would not significantly change binary orbital separations after the circularization, because the separations are regulated by q_{ij} at the trapping when the inflation has not been caused.

3.3. Formation rate of binary planets

We summarize the results of four sets of 100 runs with initial stellarcentric semi-major axes $a_1 = 1, 3, 5,$ and 10 AU (set 1, 3, 5 and 10) for $R_i = 2R_{\text{J}}$, in Fig. 6 and Table 1. The ejection rate increases and the collision one decreases as stellarcentric semimajor axis increases, because R_i/r_{Hill} decreases with the semimajor axis. The important result is that the formation rate of the binary planets is $\sim 10\%$, almost independent of the semi-major axis (in other words, almost independent of the value of R_i/r_{Hill}) as long as $a_1 = 1-10$ AU.

Compared with the results of two-planet systems, the binary formation rate is lower, because the initial conditions of two planet simulations cause tidal capture before stellarcentric eccentricity is excited. In the three planet cases, the orbital behaviors leading to tidal capture is much more complicated than in the the two planet systems and eccentricity is excited enough before the capture that the frequency of close encounters with relatively low relative velocity is diminished. Nevertheless, the formation probability of the binary planets in three planet systems is still as large as $\sim 10\%$.

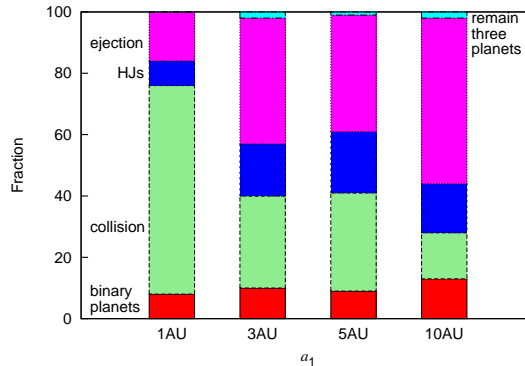


Fig. 6.— The results of 400 runs for four kinds of initial semi-major axes $a_1 = 1, 3, 5,$ and 10 AU. The colors represent binary planets (red), collision (light green), hot jupiters (blue), ejection (magenta), and remain three planets (light blue).

In order to check how the formation rate of the binary planets depends on other parameters, we carried out four additional calculations (set 0.5a, 3a, 3b, and 5a in Table 1). In these additional calculations, we changed one of the parameters (planetary radius, initial planet-planet distances, or the tidal limit) and keep the other parameters including planetary masses the same. In set 0.5a, we used half-sized planets ($R_i = 1R_{\text{J}}$), keeping the planetary masses the same. Since $a_1 = 0.5\text{AU}$, this set has the same value of R_i/r_{Hill} as set 1. As a result, the ejection/collision ratio is similar, as shown in Table 1. Although the effect of tidal dissipation is weaker than in set 1, we found that a similar (9/100) binary formation rate. The binary planets are formed through grazing encounters. When we use the smaller planetary radius, while the tidal dissipation becomes weaker, some fraction of the close encounters that lead to collisions for $R_i = 2R_{\text{J}}$ result in binary formation. These two effects tend to cancel, so that we did not find a large difference between set 1 and set 05a in our small number of statistics.

In set 3a ($a_1 = 3\text{AU}$), while we keep $R_1 = 2R_{\text{J}}$, R_2 and R_3 were reduced to $1R_{\text{J}}$. The distribution of semi-major axes of half-sized binary planets is peaked at $a_{\text{bi}} \sim 2.5R_{\text{tot}}$, which is similar to Fig. 4. However, the formation rate of the binary planets is increased to be $\sim 17\%$. The increase comes from formation of $2R_{\text{J}} - 1R_{\text{J}}$ binaries (11% of the 17%).

This may be because the $2R_J$ can suffer stronger tidal forces without collisions.

In set 3b ($a_1 = 3\text{AU}$), the planet-planet initial orbital separation set to be $\sim 6r_{\text{Hill}}$ at $a_1 = 3\text{AU}$, which is 1.5 times larger than the standard cases. Table 1 shows that the formation probability of binary planets is slightly lower ($\sim 6\%$). This is because the planets have to build up larger eccentricities for close encounters to occur and accordingly the relative velocities are higher.

In set 5a ($a_1 = 5\text{AU}$), we increased the threshold distance inside which the tidal force is incorporated, by five times at $a_1 = 5\text{AU}$. The formation probability of the binary planets does not change, as we mentioned in §3.2.

3.4. The stability of binary planets against long-term evolution due to stellar and planetary quasi-static tides

In previous sections, we showed that the binary gas giant planets are formed through the scattering of three planets orbiting around a central star and planet-planet dynamical tide with non-negligible probability ($\sim 10\%$). After the orbital circularization, the dynamical tide diminishes and the orbital evolution of the binary system is governed by long-term quasi-static tides. In this section we calculate long-term tidal evolution of the formed binary systems through the planet-planet and planet-star *quasi-static* tidal interactions, instead of dynamical tide that have been considered in previous sections. The evolution on main-sequence lifetime of solar type stars ($\sim 10\text{Gyrs}$) is very important for detectability of binary planets in extrasolar planetary systems by, e.g., transit observations (see Paper II).

We calculate this tidal evolution process, basically following Sasaki et al. (2012). Sasaki et al. (2012) neglected the tidal interactions between the central star and the binary companion and their spins. Because we consider binary planets with relatively small stellarcentric radius where the detectability by transit observation is not too small, we include all the tidal interactions and the spin angular momenta in the planet-companion-star systems.

Although we consider a pair of comparable planets, we call one planet "primary" and the other "companion" for convenience. We use the

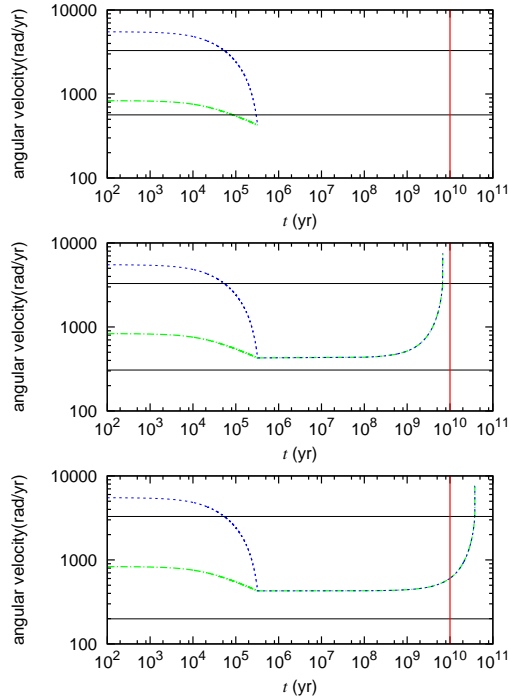


Fig. 7.— The orbital evolutions of the binary planet at $a_G = 0.2\text{AU}$ (upper panel), 0.3AU (middle panel), and 0.4AU (lower panel). The dash-dotted green line represents orbital mean motion of the binary planet, the dashed blue line shows the spin rates of planets, the vertical red lines represent the lifetime of the solar system ($t = 10^{10}\text{yr}$), the upper horizontal black line shows the orbital angular velocity of the contact binary $\sqrt{G(M_{\text{pp}} + M_{\text{cp}})/(R_{\text{pp}} + R_{\text{cp}})^3}$, and the lower horizontal black line is the critical orbital angular velocity n_{crit} .

subscripts "*" for the central star, "pp" for the primary planet, and "cp" for the companion planet. In this subsection, we use the following assumptions:

1. The total angular momentum, that is, the sum of the angular momenta of the stellar and the planets' spins and those of the binary and stellarcentric orbits, is conserved.
2. All orbits in the system are circular and coplanar.
3. All the spin angular momentum vectors are parallel to their orbital angular momentum

vectors.

4. The separation of two objects can be changed only by the tidal interactions between them and those with the host star. It is not affected by the other objects.
5. The masses of the planets are negligible compared with that of the central star, i.e., $M_* \gg M_{\text{pp}}, M_{\text{cp}}$.

The parameters we adopt in the calculations are shown in Table 2. We set $t = 0$ at the completion of tidal circularization of the binary. We assume that the initial planetary and stellar spin periods are 10 hours and 30 days, respectively. The binary orbital period is calculated by a_{bi} ; it is about 3 days for $a_{\text{bi}} = 2.5R_{\text{tot}}$. The stellarcentric orbital period is calculated by its semimajor axis of the binary barycenter; it is 1 year for $a_{\text{G}} = 1$ AU. Thus, it is reasonable to assume that $\Omega_{\text{pp}} = \Omega_{\text{cp}} > n_{\text{bi}} > n_{\text{G}}$ at $t = 0$, where Ω_{pp} and Ω_{cp} are the planetary spin frequency, n_{bi} and n_{G} are mean motions of binary and stellarcentric orbits, which are given by

$$n_{\text{bi}} = \sqrt{\frac{G(M_{\text{pp}} + M_{\text{cp}})}{a_{\text{bi}}^3}}, \quad (5)$$

$$n_{\text{G}} = \sqrt{\frac{G(M_* + M_{\text{pp}} + M_{\text{cp}})}{a_{\text{G}}^3}}. \quad (6)$$

In Appendix A, the quasi-static tidal torque equations are integrated to give $n_{\text{G}}(t)$, $n_{\text{bi}}(t)$, $\Omega_*(t)$, $\Omega_{\text{pp}}(t)$ ($= \Omega_{\text{cp}}(t)$) as explicit functions of time t :

$$n_{\text{G}}(t) = \left[\frac{39}{2} \frac{1}{G(M_{\text{pp}} + M_{\text{cp}})(GM_*)^{2/3}} \times \left(\frac{k_{2\text{pp}} R_{\text{pp}}^5}{Q_{\text{pp}}} + \frac{k_{2\text{cp}} R_{\text{cp}}^5}{Q_{\text{cp}}} + \frac{M_{\text{pp}}^2 + M_{\text{cp}}^2}{M_*^2} \frac{k_{2*} R_*^5}{Q_*} \right) t + n_{\text{G},0}^{-13/3} \right]^{-3/13}, \quad (7)$$

$$n_{\text{bi}}(t) = \left[\frac{39}{2} \frac{1}{\{G(M_{\text{pp}} + M_{\text{cp}})\}^{5/3}} \frac{1}{M_{\text{pp}} M_{\text{cp}}} \times \left(\frac{k_{2\text{pp}} R_{\text{pp}}^5 M_{\text{cp}}^2}{Q_{\text{pp}}} + \frac{k_{2\text{cp}} R_{\text{cp}}^5 M_{\text{pp}}^2}{Q_{\text{cp}}} \right) t + n_{\text{bi},0}^{-13/3} \right]^{-3/13}, \quad (8)$$

$$\begin{aligned} \Omega_*(t) &= -\frac{k_{2*} R_*^3}{\alpha_* Q_*} \frac{M_{\text{pp}} + M_{\text{cp}}}{M_*} \frac{(GM_{\text{pp}})^2 + (GM_{\text{cp}})^2}{(GM_*)^{4/3}} \\ &\times \{n_{\text{G}}^{-1/3}(t) - n_{\text{G},0}^{-1/3}\} \\ &\times \left[\frac{k_{2\text{pp}} R_{\text{pp}}^5}{Q_{\text{pp}}} + \frac{k_{2\text{cp}} R_{\text{cp}}^5}{Q_{\text{cp}}} \right. \\ &\quad \left. + \left\{ \left(\frac{M_{\text{pp}}}{M_*} \right)^2 + \left(\frac{M_{\text{cp}}}{M_*} \right)^2 \right\} \frac{k_{2*} R_*^5}{Q_*} \right]^{-1} \\ &+ \Omega_{*,0}, \end{aligned} \quad (9)$$

$$\begin{aligned} \Omega_{\text{pp}}(t) &= \Omega_{\text{cp}}(t) \\ &= -\frac{k_{2\text{pp}} R_{\text{pp}}^3}{\alpha_{\text{pp}} Q_{\text{pp}} M_{\text{pp}}} \left[\frac{(GM_{\text{pp}}) M_{\text{cp}}^3}{\{G(M_{\text{pp}} + M_{\text{cp}})\}^{1/3}} \right. \\ &\times \{n_{\text{bi}}^{-1/3}(t) - n_{\text{bi},0}^{-1/3}\} \\ &\times \left(\frac{M_{\text{cp}}^2 k_{2\text{pp}} R_{\text{pp}}^5}{Q_{\text{pp}}} + \frac{M_{\text{pp}}^2 k_{2\text{cp}} R_{\text{cp}}^5}{Q_{\text{cp}}} \right)^{-1} \\ &+ (M_{\text{pp}} + M_{\text{cp}})(GM_*)^{2/3} \{n_{\text{G}}^{-1/3}(t) - n_{\text{G},0}^{-1/3}\} \\ &\times \left[\frac{k_{2\text{pp}} R_{\text{pp}}^5}{Q_{\text{pp}}} + \frac{k_{2\text{cp}} R_{\text{cp}}^5}{Q_{\text{cp}}} \right. \\ &\quad \left. + \left\{ \left(\frac{M_{\text{pp}}}{M_*} \right)^2 + \left(\frac{M_{\text{cp}}}{M_*} \right)^2 \right\} \frac{k_{2*} R_*^5}{Q_*} \right]^{-1} \\ &+ \Omega_{\text{pp},0}, \end{aligned} \quad (10)$$

where the subscripts ",0" represent the values at $t = 0$, k_2 's are Love numbers, and Q 's are tidal dissipation functions. We adopt the estimate for the current Solar and Jovian values of k_2 and Q as parameter values of the host star and the planets, which are shown in Table 2.

Using these equations, we show in Fig. 7 the orbital evolutions of binaries at $a_{\text{G}} = 0.2$ AU (upper panel), 0.3 AU (middle panel), and 0.4 AU (lower panel). The dash-dotted green and dashed blue lines represent n_{bi} and Ω_{pp} . The vertical red lines represent the lifetime of main sequence phase of solar-type stars ($t = 10^{10}$ yr), the upper horizontal black lines are the binary orbital angular velocities for a contact binary ($[G(M_{\text{pp}} + M_{\text{cp}})/(R_{\text{pp}} + R_{\text{cp}})^3]^{1/2}$), and the lower one represents n_{crit} that is determined by the critical semi-major axis of the binary orbit, below which the binary separation is so large that the orbit is destabilized by stellar gravitational force (eq.

	α	k_2	Q	References
Sun	0.059	0.002	10^6	Goldreich & Soter (1966); Yoder (1995)
Jupiter	0.254	0.5	10^5	Sasaki et al. (2012)

Table 2: The tidal parameters of the Sun and the Jupiter: moment of inertia ratios α , Love numbers k_2 , and tidal dissipation functions Q .

[A17]). When the dash-dotted green lines stay in the region surrounded two horizontal black lines ($n_{\text{crit}} < n_{\text{bi}} < [G(M_{\text{pp}} + M_{\text{cp}})/(R_{\text{pp}} + R_{\text{cp}})]^{1/2}$) the binary planets are stable. The two planets collide for $n_{\text{bi}} \geq [G(M_{\text{pp}} + M_{\text{cp}})/(R_{\text{pp}} + R_{\text{cp}})]^{1/2}$ and they escape from each other for $n_{\text{bi}} \leq n_{\text{crit}}$.

The spins of the individual planets are slowed down by the planet-planet tidal interaction and accordingly the binary orbital angular momentum is increased. As a result, both $\Omega_{\text{pp}}(t)$ and $n_{\text{bi}}(t)$ decrease. Since $\Omega_{\text{pp}}(t)$'s deceleration is faster than that of $n_{\text{bi}}(t)$, $\Omega_{\text{pp}}(t)$ catches up with $n_{\text{bi}}(t)$ to establish a synchronous state. After that, the binary planets keep the synchronized state while $n_{\text{G}}(t)$ is decelerated by the tidal torque from the star. In this synchronous state with $\Omega_{\text{pp}} = \Omega_{\text{cp}} = n_{\text{bi}}$, the total angular momentum is given by

$$\begin{aligned}
L &= L_{\text{bi}} + L_{\text{G}} + I_*\Omega_* + I_{\text{pp}}\Omega_{\text{pp}} + I_{\text{cp}}\Omega_{\text{cp}}, \quad (11) \\
&= \frac{M_{\text{cp}}(GM_{\text{pp}})}{\{n_{\text{bi}}G(M_{\text{pp}} + M_{\text{cp}})\}^{1/3}} \\
&\quad + \frac{(M_{\text{pp}} + M_{\text{cp}})(GM_*)^{2/3}}{n_{\text{G}}^{1/3}} \\
&\quad + \alpha_*R_*^2M_*\Omega_* \\
&\quad + (\alpha_{\text{pp}}R_{\text{pp}}^2M_{\text{pp}} + \alpha_{\text{cp}}R_{\text{cp}}^2M_{\text{cp}})n_{\text{bi}}, \quad (12)
\end{aligned}$$

where α 's are moment of inertia ratios, the values of which we adopted are shown in Table 2. Since L_{G} ($\propto n_{\text{G}}(t)^{-1/3}$) increases continuously, $\Omega_{\text{pp}}(t)$ and $n_{\text{bi}}(t)$ increase to keep the synchronized state from the total angular momentum conservation (L_{bi} and $I_*\Omega_*$ decrease, but L_{G} , $I_{\text{pp}}\Omega_{\text{pp}}$, and $I_{\text{cp}}\Omega_{\text{cp}}$ increase). Because $n_{\text{bi}}(t)$ keeps increasing, a_{bi} keeps decreasing and eventually the binary planets collide with each other.

The synchronous state among Ω_{pp} , Ω_{cp} , and n_{bi} is established in about 0.3 Myr in the cases of $a_{\text{G}} = 0.3$ AU and 0.4 AU. However, in the case of $a_{\text{G}} = 0.2$ AU, it becomes $n_{\text{bi}} < n_{\text{crit}}$ and two planets escape from each other in about 0.1 Myr before the synchronous state is established. The lifetime

of the binary planets is longer than main-sequence phase of solar-type stars (~ 10 Gyrs) for $a_{\text{G}} = 0.4$ AU. For $a_{\text{G}} = 0.3$ AU, the lifetime is about 7 Gyrs. But, since the tidal torque is proportional to fifth-order of the planetary radius (equation [A1]), the lifetime for $R_{\text{pp}}, R_{\text{cp}} = 1R_{\text{J}}$ with the same $M_{\text{pp}}, M_{\text{cp}} = 1M_{\text{J}}$ is lengthened by about 10 times from that in this plot. Because gas envelope may fully contract in 0.1 Gyr, $R_{\text{pp}}, R_{\text{cp}} = 1R_{\text{J}}$ may be more appropriate than $2R_{\text{J}}$ for the estimate of the binary lifetime. Thereby, the binary would survive also for $a_{\text{G}} = 0.3$ AU.

We adopted 10 hours as the initial planetary spin periods, $2\pi/\Omega_{\text{pp},0}$ and $2\pi/\Omega_{\text{cp},0}$. For smaller $\Omega_{\text{pp},0}$ and $\Omega_{\text{cp},0}$, the lifetime of the binary is shorter, but the lifetime is still ~ 20 Gyr for $a_{\text{G}} = 0.4$ AU even if $\Omega_{\text{pp},0} = n_{\text{bi},0}$. On the other hand, when the planetary spin period is $\lesssim 4$ hours, the binary is separated more than a_{crit} before reaching the synchronous state.

The Q value may include large uncertainty. However, the binary stability condition for a_{G} comes from the tidal evolution timescale due to stellar tide compared with 10 Gyrs. Since the timescale is proportional to $Q_{\text{pp}}a_{\text{G}}^{6.5}$ (Eq. A20), the condition for a_{G} is not severely affected by the uncertainty in the Q value.

Note also that we neglect the spins in planet-planet scattering calculations. The planetary spin axis can be reversed in scattering. The binary approaches and impacts each other quickly by tidal evolution when binary orbit and spin are retrograde. When stellarcentric orbit and binary orbit are retrograde, the 1st, 4th, and 5th terms in equation (11) change their signs and the binary is separated away. That means even if $a_{\text{G}} \gtrsim 0.3$ AU, a part of the binary planets cannot survive.

4. CONCLUSIONS

In this paper, we have studied the formation of binary planets (a gravitationally bound pair

of planets like a planet-satellite system) by the capture due to planet-planet *dynamical* tide during orbital crossing of three giant planets and the following long-term evolution due to *quasi-static* planet-planet and planet-star tides.

The scattering of three giant planets usually ends up with ejection, a collision between planets, or a collision with the central star. Nagasawa et al. (2008) have found that some fraction of paths to collisions with the central star can be replaced by formation of a hot jupiter if planet-star tidal interaction is included. Here, we have pointed out that some fraction of collisions between planets are replaced by formation of the binary planets if planet-planet tidal interaction is incorporated.

Through N-body simulations taking into account planet-planet and planet-star tidal interactions (dynamical tide), we have found the followings:

1. The binary planets are formed in $\sim 10\%$ of the three planet systems that undergo orbital crossing. The fraction is independent of stellarcentric orbital radius (at least in a range of 0.5 AU – 10 AU that we examined). Although the formation probability is lower than that found in optimized two planet setting by Podsiadlowski et al. (2010), it is still non-negligible. Since our initial settings are much more realistic, the 10% probability encourages observational detection.
2. The binary planets tend to be formed in early stage of orbital instability. In fact, almost all binary planets are formed around their original locations.
3. Initial captures usually occur at separations of $\sim 1 - 2$ times of the sum of planetary radii $R_{\text{tot}} = (R_i + R_j)$, resulting in highly eccentric orbits with a pericenter distance of $\sim (1 - 2)R_{\text{tot}}$ after the trapping. Through tidal circularization, the pericenter distance expands by a factor of 2 because of the conservation of the binary’s angular momentum. Finally, binary planets with separations of $\sim (2 - 4)R_{\text{tot}}$ are formed.

Because dynamical tide diminishes as eccentricity of the binary orbits decreases, subsequent orbital evolution is dominated by long-term quasi-static tides. We studied the long-term evolution of the formed binary planets, taking into account planet-planet and planet star quasi-static tidal interactions. We found that

4. If the stellarcentric semimajor axis is larger than 0.3 AU, the binary is not destroyed during main sequence lifetime of solar type stars ($\sim 10^{10}$ years).

During the long-term tidal evolution, we have neglected the effect of a third planet. It is very rare that the third one enters the Hill sphere of the binary and the third one hardly affects the binary tidal evolution. Gong et al. (2013) showed that even if a loosely bounded satellite with a separation $\sim 0.1r_{\text{Hill}}$ survives strong orbital scattering by another planet with $\sim 20\%$ of probability.

Since we can predict a frequency of binary planets, binary separations and a range of stellarcentric semimajor axis where binary planets exist, we are greatly interested in detectability of extrasolar binary planets. Ochiai et al. (2014, Paper II) concludes that among various observational methods, detecting modulations of transit light curves is the most promising. If radial velocity follow-up can determine the mass of the bodies, the bulk density derived by assuming a hypothetical single planet would be $\sqrt{2}$ times lower than the real bulk density of binary planets. Thereby, some of objects classified as inflated gas giants or false positives could be binary planets. We will discuss these observation issues in details in Paper II.

We thank Takahiro Sumi, Karen Lewis, Tristan Guillot and Rosemary Mardelling for discussions on observations of binary planets. We also thank Takayuki Tanigawa and Hidenori Genda for helpful theoretical comments. This research was supported by a grant for JSPS (23103005) Grant-in-aid for Scientific Research on Innovative Areas.

A. Long-term evolution due to quasi-static tides

We calculate the tidal evolution of the star-primary-companion system following Sasaki et al. (2012). The torque exerted on the object i from the object j is given by Murray & Dermott (1999) as

$$\tau_{i-j} = -\frac{3}{2} \frac{Gk_{2i}R_i^5M_j^2}{Q_ia_j^6} \text{sgn}(\Omega_i - n_j), \quad (\text{A1})$$

where n_j is the orbital mean motion of the object j around the object i and Ω_i is its spin angular velocity.

Here we consider a pair of comparable planets. But, we call one planet "primary" and the other "companion" for convenience, and use the subscripts "*" for the central star, "pp" for the primary planet, and "cp" for the companion planet. The total angular momentum L is

$$L = L_{\text{bi}} + L_{\text{G}} + I_*\Omega_* + I_{\text{pp}}\Omega_{\text{pp}} + I_{\text{cp}}\Omega_{\text{cp}}, \quad (\text{A2})$$

where $I_i = \alpha_i R_i^2 M_i$ is the inertia moment of the object i and

$$L_{\text{G}} = (M_{\text{pp}} + M_{\text{cp}}) \sqrt{G(M_* + M_{\text{pp}} + M_{\text{cp}})a_{\text{G}}} = \frac{(M_{\text{pp}} + M_{\text{cp}})(GM_*)^{2/3}}{n_{\text{G}}^{1/3}(t)}, \quad (\text{A3})$$

$$L_{\text{bi}} = \frac{M_{\text{pp}}M_{\text{cp}}}{M_{\text{pp}} + M_{\text{cp}}} \sqrt{G(M_{\text{pp}} + M_{\text{cp}})a_{\text{bi}}} = \frac{M_{\text{cp}}(GM_{\text{pp}})}{\{G(M_{\text{pp}} + M_{\text{cp}})n_{\text{bi}}(t)\}^{1/3}}, \quad (\text{A4})$$

are the angular momenta of stellarcentric and the binary orbits, respectively (where we use equations (5) and (6) and the assumption 5 in §3.4).

Sasaki et al. (2012) neglected the interactions between the central star and the companion planet (in their case, "moon") and their spins. Since we also consider the binary planets with relatively small stellarcentric orbital radius where the transit detectability are high, we include all the tidal interactions and the spin angular momenta in the star-planet-companion system. The spin and angular momenta change rates are written as

$$I_* \frac{d\Omega_*}{dt} = \tau_{*-pp} + \tau_{*-cp}, \quad (\text{A5})$$

$$I_{\text{pp}} \frac{d\Omega_{\text{pp}}}{dt} = \tau_{\text{pp-cp}} + \tau_{\text{pp-*}}, \quad (\text{A6})$$

$$I_{\text{cp}} \frac{d\Omega_{\text{cp}}}{dt} = \tau_{\text{cp-pp}} + \tau_{\text{cp-*}}, \quad (\text{A7})$$

$$\frac{dL_{\text{G}}}{dt} = -\tau_{*-pp} - \tau_{\text{pp-*}} - \tau_{*-cp} - \tau_{\text{cp-*}}, \quad (\text{A8})$$

$$\frac{dL_{\text{bi}}}{dt} = -\tau_{\text{pp-cp}} - \tau_{\text{cp-pp}}, \quad (\text{A9})$$

where we use the assumption 4 in §3.4.

We calculated the tidal evolution using above equations. From the time derivations of equations (A3) and (A4), we derived

$$\frac{dn_{\text{G}}}{dt} = -\frac{3}{(M_{\text{pp}} + M_{\text{cp}})(GM_*)^{2/3}} n_{\text{G}}^{4/3}(t) \frac{dL_{\text{G}}}{dt}, \quad (\text{A10})$$

$$\frac{dn_{\text{bi}}}{dt} = -\frac{3\{G(M_{\text{pp}} + M_{\text{cp}})\}^{1/3}}{M_{\text{cp}}(GM_{\text{pp}})} n_{\text{bi}}^{4/3}(t) \frac{dL_{\text{bi}}}{dt}, \quad (\text{A11})$$

and the integrations of these equations gives

$$n_{\text{G}}(t) = \left[\frac{39}{2} \frac{1}{G(M_{\text{pp}} + M_{\text{cp}})(GM_*)^{2/3}} \left(\frac{k_{2\text{pp}}}{Q_{\text{pp}}} R_{\text{pp}}^5 + \frac{k_{2\text{cp}}}{Q_{\text{cp}}} R_{\text{cp}}^5 + \frac{M_{\text{pp}}^2 + M_{\text{cp}}^2}{M_*^2} \frac{k_{2*}}{Q_*} R_*^5 \right) t + n_{\text{G},0}^{-13/3} \right]^{-3/13},$$

(A12)

$$n_{\text{bi}}(t) = \left[\frac{39}{2} \frac{1}{\{G(M_{\text{pp}} + M_{\text{cp}})\}^{5/3}} \frac{1}{M_{\text{pp}}M_{\text{cp}}} \left(\frac{k_{2\text{pp}}}{Q_{\text{pp}}} R_{\text{pp}}^5 M_{\text{cp}}^2 + \frac{k_{2\text{cp}}}{Q_{\text{cp}}} R_{\text{cp}}^5 M_{\text{pp}}^2 \right) t + n_{\text{bi},0}^{-13/3} \right]^{-3/13}, \quad (\text{A13})$$

where the subscripts ",0" represent the values at $t = 0$, k_2 's are Love numbers, and Q 's are quality Q factors.

The spin angular velocities are derived from the similar methods as

$$\begin{aligned} \Omega_*(t) &= -\frac{k_{2*} R_*^3}{\alpha_* Q_*} \frac{M_{\text{pp}} + M_{\text{cp}}}{M_*} \frac{(GM_{\text{pp}})^2 + (GM_{\text{cp}})^2}{(GM_*)^{4/3}} \\ &\times \frac{\{n_{\text{G}}^{-1/3}(t) - n_{\text{G},0}^{-1/3}\}}{\left[k_{2\text{pp}} R_{\text{pp}}^5 / Q_{\text{pp}} + k_{2\text{cp}} R_{\text{cp}}^5 / Q_{\text{cp}} + \{(M_{\text{pp}}/M_*)^2 + (M_{\text{cp}}/M_*)^2\} k_{2*} R_*^5 / Q_* \right]} \\ &+ \Omega_{*,0}, \end{aligned} \quad (\text{A14})$$

$$\begin{aligned} \Omega_{\text{pp}}(t) &= \Omega_{\text{cp}}(t) = -\frac{k_{2\text{pp}} R_{\text{pp}}^3}{\alpha_{\text{pp}} Q_{\text{pp}} M_{\text{pp}}} \\ &\times \left\{ \frac{(GM_{\text{pp}}) M_{\text{cp}}^3}{\{G(M_{\text{pp}} + M_{\text{cp}})\}^{1/3}} \frac{n_{\text{bi}}^{-1/3}(t) - n_{\text{bi},0}^{-1/3}}{(M_{\text{cp}}^2 k_{2\text{pp}} R_{\text{pp}}^5 / Q_{\text{pp}} + M_{\text{pp}}^2 k_{2\text{cp}} R_{\text{cp}}^5 / Q_{\text{cp}})} \right. \\ &+ \left. \frac{(M_{\text{pp}} + M_{\text{cp}})(GM_*)^{2/3} \{n_{\text{G}}^{-1/3}(t) - n_{\text{G},0}^{-1/3}\}}{\left[k_{2\text{pp}} R_{\text{pp}}^5 / Q_{\text{pp}} + k_{2\text{cp}} R_{\text{cp}}^5 / Q_{\text{cp}} + \{(M_{\text{pp}}/M_*)^2 + (M_{\text{cp}}/M_*)^2\} k_{2*} R_*^5 / Q_* \right]} \right\} \\ &+ \Omega_{\text{pp},0}. \end{aligned} \quad (\text{A15})$$

When the spins of the binary planets become synchronous with the binary orbital rotation, we can write $\Omega_{\text{pp}} = \Omega_{\text{cp}} = n_{\text{bi}}$. From the total angular momentum conservation,

$$\begin{aligned} L(t \geq \tau_1) &= \frac{M_{\text{cp}}(GM_{\text{pp}})}{\{n_{\text{bi}}(t)G(M_{\text{pp}} + M_{\text{cp}})\}^{1/3}} + \frac{(M_{\text{pp}} + M_{\text{cp}})(GM_*)^{2/3}}{n_{\text{G}}^{1/3}(t)} \\ &+ \alpha_* R_*^2 M_* \Omega_*(t) + (\alpha_{\text{pp}} R_{\text{pp}}^2 M_{\text{pp}} + \alpha_{\text{cp}} R_{\text{cp}}^2 M_{\text{cp}}) n_{\text{bi}}(t), \end{aligned} \quad (\text{A16})$$

where $t = \tau_1$ is the time when the synchronous state begins.

However, the binary planets become unstable if the binary separation becomes large enough before they are tidally rocked. The critical semi-major axis of the binary orbit (a_{crit}), beyond which the binary orbit is destabilized by stellar gravitational force is

$$a_{\text{crit}} = f r_{\text{Hill}} = f \left(\frac{M_{\text{pp}} + M_{\text{cp}}}{3M_*} \right)^{1/3} a_{\text{G}}. \quad (\text{A17})$$

We take $f = 0.36$ following Sasaki et al. (2012). The binary orbit becomes unstable, when

$$n_{\text{bi}}(t) < n_{\text{crit}} \equiv \sqrt{\frac{G(M_{\text{pp}} + M_{\text{cp}})}{a_{\text{crit}}^3}}. \quad (\text{A18})$$

The timescale of the binary's tidal evolution is

$$\begin{aligned} \tau_1 &\sim \frac{n_{\text{bi}}}{dn_{\text{bi}}/dt} = -\frac{1}{3} \frac{L_{\text{bi}}}{dL_{\text{bi}}/dt} = \frac{1}{9} \frac{1}{\sqrt{2GM_{\text{pp}}}} \frac{Q_{\text{pp}}}{k_{2\text{pp}} R_{\text{pp}}^5} a_{\text{bi}}^{6.5} \\ &\sim 10^5 \left(\frac{a_{\text{bi}}}{5R_{\text{pp}}} \right)^{6.5} \text{ yr}, \end{aligned} \quad (\text{A19})$$

where the physical parameters of the planets are the same. Taking the major term of equation (A8), the timescale of tidal evolution of binary's barycenter τ_2 is derived by the similar method as

$$\begin{aligned}\tau_2 &\sim \frac{n_G}{dn_G/dt} = -\frac{1}{3} \frac{L_G}{dL_G/dt} \sim \frac{2}{9} \frac{1}{\sqrt{GM_*}} \frac{M_{pp}}{M_*} \frac{Q_{pp}}{k_{2pp} R_{pp}^5} a_G^{6.5} \\ &\sim 10^{16} \left(\frac{M_*}{M_\odot}\right)^{-1.5} \left(\frac{M_{pp}}{M_J}\right)^{-2/3} \left(\frac{a_G}{1\text{AU}}\right)^{6.5} \text{ yr},\end{aligned}\tag{A20}$$

which is much longer than the estimation of equation (A19).

REFERENCES

- Beaugé, C. & Nesvorný, D. 2012, *ApJ*, 751, 119
- Chambers, J. E., Wetherill, G. W., & Boss, A. P. 1996, *Icarus*, 119, 261
- Chatterjee, S., Ford, E. B., Matsumura, S., & Rasio, F. A. 2008, *ApJ*, 686, 580
- Ford, E. B. & Rasio, F. A. 2008, *ApJ*, 686, 621
- Gladman, B. 1993, *Icarus*, 106, 247
- Goldreich, P. & Soter, S. 1966, *Icarus*, 5, 375
- Gong, Y.-X. Zhou, J.-L. Xie, J.-W., & Wu, X. M. 2013, *ApJL*, 769, L14
- Ikoma, T., Guillot, T., Genda, H., Tanigawa, T., & Ida, S. 2006, *ApJ*, 650, 1150
- Jurić, M. & Tremaine, S. 2008, *ApJ*, 686, 603
- Lega, E., Morbidelli, A., & Nesvorný D. 2013, *MNRAS*, 431, 3494
- Lin, D. N. C & Ida, S. 1997, *ApJ*, 477, 781
- Mardling, R. A. 1995, *ApJ*, 450, 732
- Marzari, F. & Weidenschilling, S. J. 2002, *Icarus*, 156, 570
- Murray, C. D. & Dermott, S. F. 1999, *Solar System Dynamics* (Cambridge: Cambridge Univ. Press)
- Nagasawa, M., Ida, S., & Bessho, T. 2008, *ApJ*, 678, 498
- Nagasawa, M. & Ida, S. 2011, *ApJ*, 742, 72
- Ochiai, H., Lewis, K. M., Nagasawa, M., & Ida, S. 2014, submitted (Paper II)
- Podsiadlowski, P., Rappaport, S., Fregeau J. M., & Mardling, R. A. 2010, arXiv:1007.1418
- Portegies Zwart, S. F. & Meinen, A. T. 1993, *A&A*, 280, 174
- Press, W. H. & Teukolsky, S. A. 1977, *ApJ*, 213, 183
- Rasio, F. A. & Ford, E. B. 1996, *Science*, 274, 954
- Sasaki, T., Barnes, J. W., & O'Brien, D. P. 2012, *ApJ*, 754, 51
- Weidenschilling, S. J. & Marzari, F., 1996, *Nature*, 384, 619
- Yoder, C. F. 1995, *Astrometric and Geodetic Properties of Earth and the Solar System*, (Washington, D.C.: American Geophysical Union)